2-11-2008

Mitral Cell Dendritic Development in the Mouse Main Olfactory Bulb

Masha Rand Diede
Yale University

MITRAL CELL DENDRITIC DEVELOPMENT IN THE MOUSE MAIN OLFACTORY BULB

A Thesis Submitted to the

Yale University School of Medicine

in Partial Fulfillment of the Requirements for the

Degree of Doctor of Medicine

by

Masha Rand Diede

2007

ABSTRACT

Mitral cell dendritic development in the mouse main olfactory bulb.

Masha Rand Diede and Charles A. Greer. Department of Neurosurgery, Yale University, School of Medicine, New Haven, CT.

Correct targeting and differentiation of the mitral cell (MC) dendrites in the olfactory bulb (OB) is clearly essential for development of functional neuronal circuits. MCs, the primary OB projection neurons, receive odor information from OSN axons via axodendritic synapses on their apical dendrite; the signal is further processed via dendrodendritic synapses on MC lateral dendrites. In the adult, each MC cell apical dendrite targets a single glomerulus, ending in a characteristic glomerular tuft and receiving input from molecularly defined subsets of OSNs. MC lateral dendrites segregate deep to the glomerular layer, in a sublamina of the external plexiform layer. MC dendrites are initially undifferentiated and often supernumerary; the adult form of one apical and several lateral dendrites emerges postnatally. We sought to define more clearly the emergence of MC apical versus lateral dendrites using DiI fills. We also used a dendritic growth cone specific antibody, CDA 1 to assess spatiotemporal patterns of development in the OB.

MCs progressed through a broad spectrum of transitional morphologies – from a broadly spread arbor of supernumerary dendrites in the embryo to the single apical dendrite and lateral dendrites characteristic of the adult. At P0, MCs exhibit the immature dendritic morphology with a broadly spread arbor of a large number of relatively uniform dendrites. By P1, this arbor appears to have narrowed and one dendrite appears thicker than the others, probably on its way to differentiating into an apical dendrite. At P4, two clearly distinguishable subpopulations of neurons have clearly emerged, but some cells exhibit two apical dendrites. By P8, MCs appear to have an adult dendritic morphology.

Quantitative analysis of CDA 1 expression patterns in the OB at postnatal day 0, 2, 4, 8, suggests intra- and interlaminar patterns of dendritic development. Preliminary data further suggest distinct temporal windows of MC dendritic development along the rostrocaudal axis. CDA 1 expression in all laminae decreases significantly by postnatal day 8 and appears indistinguishable from background in the adult. Thus, both lines of data show evidence of significant postnatal dendritic remodeling.

ACKNOWLEDGEMENTS

I am extraordinarily fortunate to have Dr. Charles August Greer for a mentor. I cannot thank him enough for his guidance, discipline, encouragement and inspiration as a teacher as well as for his kindness and warmth as a person. In addition, I would like to express my gratitude to the entire Greer Lab for all their help and support. In particular, I am grateful to Dr. Diego Rodriguez Gil for his constant readiness to discuss and advise and for his careful reading and astute comments, Dolores Montoya for her tireless technical assistance and Dr. Helen B. Treloar for all her help. Finally, I could not have written this without my brother, Dr. Michael C. Rand.

This work was generously supported by HHHMI in conjunction with the HHMI Medical Student Research Fellowship and NIH DC00210, DC006729 and DC006291.

TABLE OF CONTENTS

INTRODUCTION

THE OLFACTORY SYSTEM

Humans are said to be able to recognize up to 10,000 distinct smells and perfumers claim to be able to discriminate as many as 5,000 different odorants (odor components). Furthermore, olfactory acuity and sensitivity are widely considered to be weaker in humans than other animals, although this position is currently being reconsidered in light of a number of new studies (for review see Shepherd, 2004). Whatever the verdict, smell is an indispensable mode of gauging and interacting with the environment for many species, essential for distinguishing friend from foe or delicious from deadly. Testimony to the importance of the olfactory system is the fact that approximately 2% of the human genome and an impressive 6% of the mouse genome are dedicated to encoding up to 1,000 olfactory receptors, i.e., the receptors responsible for actual odorant detection (Mombaerts, 2001). In other words, about one in 30 genes are dedicated to smell. Furthermore, however large the number of olfactory receptors, it is estimated that the ratio of odorants to olfactory receptors is ten to one, i.e., that approximately 10 different odorants or ligands may bind to any single olfactory receptor, though the specificity or efficacy of binding may differ across odorants. How does the central nervous system accomplish the gargantuan task of recognizing and processing this enormous array of stimuli?

The olfactory system is the component of the nervous system designed to sense, interpret and prepare a response to chemical stimuli in the environment. For terrestrial animals volatile molecules in the air constitute their odor environment, water soluble molecules are the chemical stimuli for aquatic organisms while those that divide their

time between land and sea have developed strategies for adapting their particular olfactory apparatus to both environments (Catania, 2006). It stands to reason that olfaction is ubiquitous in the animal kingdom and its organizational principles remarkably similar across species, especially among vertebrates (Ache & Young, 2005). The primary model systems in the study of olfaction have been rodents and fruit flies, though research has also been conducted in a large number of other species as well. Although there are fundamental similarities between the vertebrate and invertebrate olfactory systems, they are also different enough that I will focus my attention primarily on mammalian olfaction, most notably murine.

HISTORY OF OLFACTORY SYSTEM STUDIES

The physician and histologist Santiago Ramon y Cajal, along with other turn of the 20th century histologists, including Camillo Golgi and M.G. Retzius, helped lay the foundation for modern neuroscience in general and the study of the olfactory system more specifically with his detailed neuroanatomical descriptions of the olfactory bulb in his ground-breaking work *Histologie du Système Nerveux de l'Homme et de Vertébrés* (Cajal, 1911). In fact, he and Golgi were jointly awarded the Nobel Prize

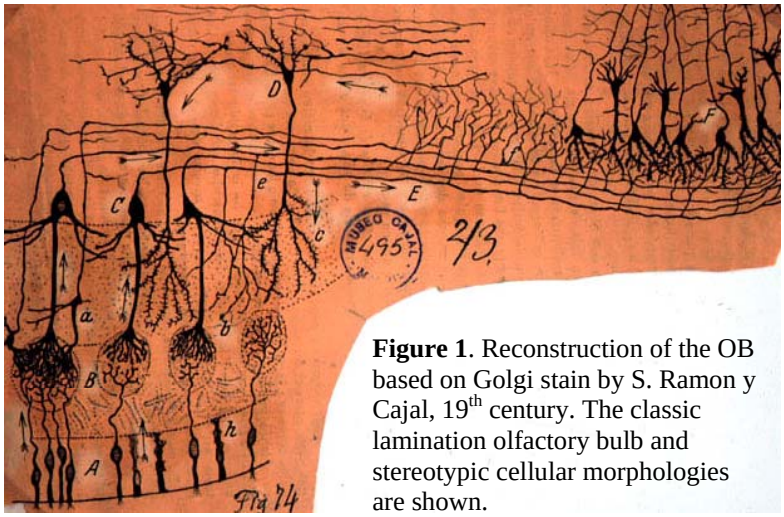

Figure 1. Reconstruction of the OB based on Golgi stain by S. Ramon y Cajal, 19th century. The classic lamination olfactory bulb and stereotypic cellular morphologies are shown.

in Medicine and Physiology in 1906 for their work on establishing the neuron doctrine, based heavily on their interpretations of organization in the olfactory system.

Seminal work in contemporary olfactory studies was done by Linda Buck and Richard Axel (Buck & Axel, 1991). Their work radically transformed our understanding of olfaction and earned them the Nobel Prize in Medicine and Physiology in 2004 (Axel, 2005; Buck, 2005). Buck, working at the time as a postdoctoral fellow in the Axel lab, initially discovered the aforementioned family of genes in the mouse encoding ≥1,000 olfactory receptors (ORs), i.e. the receptors that recognize odorants. This set the stage for taking a new approach to the olfactory code, including applying molecular and genetic techniques to the study of the receptors themselves and allowed us to begin elucidating details of the mechanism whereby the nervous system processes the thousands of different odorants with which it is presented.

BASIC OLFACTORY CIRCUIT

The olfactory pathway is a single relay circuit (figure 2). Peripheral, sensory neurons pick up and pass along odor signals to central output neurons located in the main olfactory bulb (OB), which convey the information higher processing centers in the brain. In addition to input and output components, there are intrinsic neurons within the OB involved in refining the odor signal. (For detailed reviews of the basic olfactory circuit see Shepherd *et al.*, 2004; Firestein, 2001; Buck 2005; Axel 2005).

The peripheral sensory neurons, olfactory sensory neurons (OSNs), are located in specialized olfactory epithelium (OE) in the nasal cavity (Zhang and Firestein, 2002).

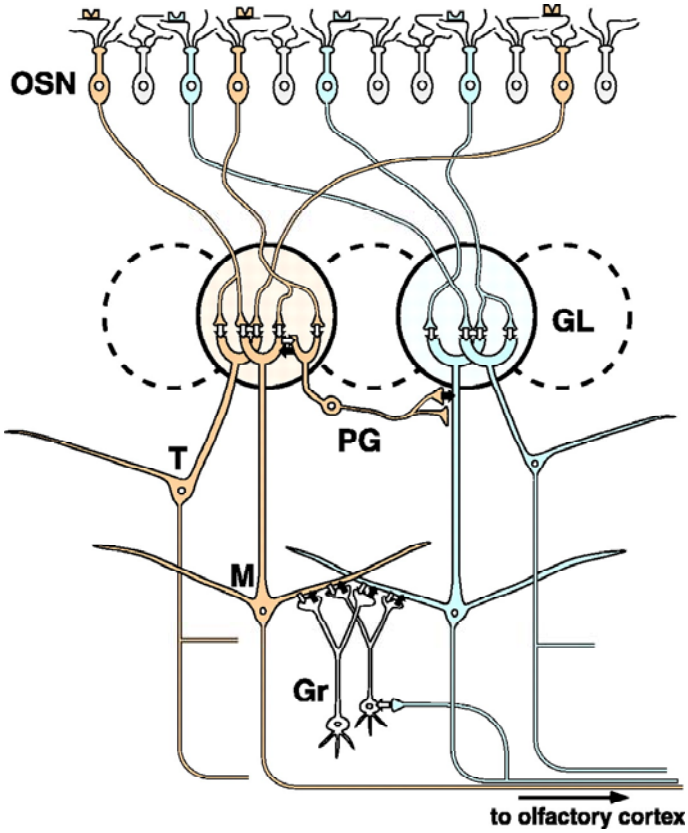

Figure 2. Olfactory Circuit. Odor ligands are transduced by olfactory sensory neurons (OSN) and conveyed via the OSN axons to the olfactory bulb where they synapse with the main 2nd order projection neurons, mitral cells (M) and tufted cells (T) within glomeruli (GL). Periglomerular cells (PG) and granule cells (GR) are intrinsic neurons involved in signal refinement via modulation of M and T cell activity. M and T cells project to the olfactory cortex, which then conveys odor related information throughout the neuraxis.

The axons of the OSNs coalesce to form the olfactory nerve (ON, cranial nerve I), which penetrates the cribiform plate of the ethmoid bone as it exits the OE and fuses on the outermost surface of the OB. Upon reaching the OB, the OSN axons exit the nerve layer and enter spherical areas of neuropil, glomeruli, where they establish excitatory axodendritic synapses with second-order projection neurons, mitral (MCs) and tufted (TCs) cells, as well as local interneurons, periglomerular cells (PGs). The projection neurons convey the information to the higher cortical regions, olfactory cortex (OC), including piriform cortex, entorhinal cortex, the olfactory tubercle, anterior olfactory nucleus (aON), as well as to the thalamus and limbic system, including several nuclei in the amygdala. MCs and TCs are also involved, along with intrinsic neurons, in modulating and refining odor-invoked activity within the bulb via feedback- and lateral-inhibition, demarcating given odor input (Shipley and Ennis,

1996). As olfactory input proceeds through the highest cortical regions, further processing occurs as well as integration with input from other sensory systems including taste and with affective quality.

The olfactory system is also under widespread central control from the brain (Shepherd *et al.*, 2004; Buck, 2005). In addition to afferent projections, the OB receives efferent or centrifugal input. This central input comes from numerous areas in the brain including, the *locus coeruleus* and *raphe nucleus* in the brainstem, the nucleus of the horizontal limb of the diagonal band in the basal forebrain, the aON, and olfactory cortex.

OLFACTORY BULB

The OB, the first step in odor signal processing and refinement, is an outgrowth of the forebrain. It is organized into six sharply demarcated laminae, each of which consists of a distinct cell population (figure 3). From outer to inner, these are: the ONL, the glomerular layer (GL), the external plexiform layer (EPL), the mitral cell layer (MCL), the internal plexiform layer (IPL) and the granule cell layer (GCL). As mentioned above, the ONL is composed of incoming OSN axons. The GL is where OSNs synapse with MCs, TCs, and PGs in anatomical and functional modules called glomeruli. Following is the EPL, which is primarily composed of MC and TC dendrites, TC cell bodies and several less well-characterized interneuron populations. The EPL is the site of significant odor signal refinement. Deep to the EPL, the MCL in the adult is composed of a monolayer of MC somata and deep to that is the IPL, containing MC and TC axon collaterals. Finally, the GCL contains granule cells another population of interneurons called short-axon cells somata and dendrites as well as also containing axon collaterals

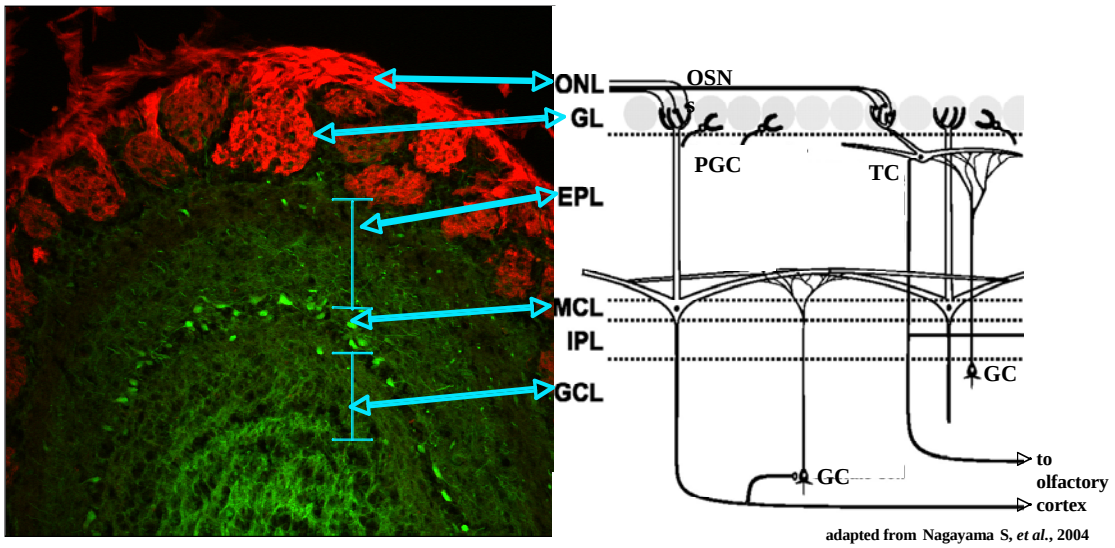

Figure 3. Laminar organization of OB. Side by side schematic and histological cross-sectional view of the OB illustrating the six OB lamina: the ONL, the glomerular layer (GL), the external plexiform layer (EPL), the mitral cell layer (MCL), the internal plexiform layer (IPL) and the granule cell layer (GCL). The ONL is composed of incoming OSN axons. OSNs synapse with MCs, TCs, and PGs in the GL within glomeruli. The EPL, which is primarily composed of MC and TC dendrites, TC cell bodies and several less well-characterized interneuron populations. Deep to the EPL, the MCL in the adult is composed of a monolayer of MC somata and deep to that is the IPL, containing MC and TC axon collaterals. The GCL contains granule cells another population of interneurons called short-axon cells somata and dendrites as well as also containing axon collaterals from MCs and TCs.

from MCs and TCs. (For a thorough summary of the structure of the OB, see Shepherd *et al.*, 2004).

In addition to laminar organization, there is extensive evidence of sublaminar organization. For example, Au *et al*. (2002) provide evidence of an outer and inner ONL and suggest that these may reflect functional division of axonal sorting and axonal targeting activity. The EPL exhibits sublaminar distribution of CCK immunoreactivity (Seroogy *et al.*, 1985), which appears to represent, in part, a restricted subpopulation of TCs that use CCK as a neurotransmitter (Liu and Shipley, 1994). The GCL has been shown to exhibit sublaminar organization in the guinea pig using neuropeptide Y immunoreactivity (Matsutani *et al.*, 1989). Finally, our research has yielded observations of sublaminar organization within the EPL.

OLFACTORY SENSORY NEURONS

There are several million OSNs located in the OE at any one time. The OE is an area of several square centimeters of specialized neuroepithelium located in the dorsal aspect of the nasal cavity (Mombaerts, 2001).

In addition, the OE contains two other major cell populations: sustenacular cells, and basal cells (figure 4). Sustenacular cells are interspersed among the OSNs and provide structural support. Basal cells are located deep to OSNs and constitute a pool of stem cells from which OSNs are regenerated approximately every few weeks (Graziadei and Monti-Graziadei, 1979). Interestingly, OSNs are one of only three currently known populations of CNS neurons that exhibit continuous regeneration throughout adulthood (others include granule cells in the OB as well as in the hippocampus (for review see Lledo *et al*., 2006). This makes the OB an attractive area for inquiry into stem cell function and nerve regeneration among other things. OSNs are a morphologically homogenous population of bipolar neurons. They have a short non-branching dendrite that extends towards the surface of the OE. The

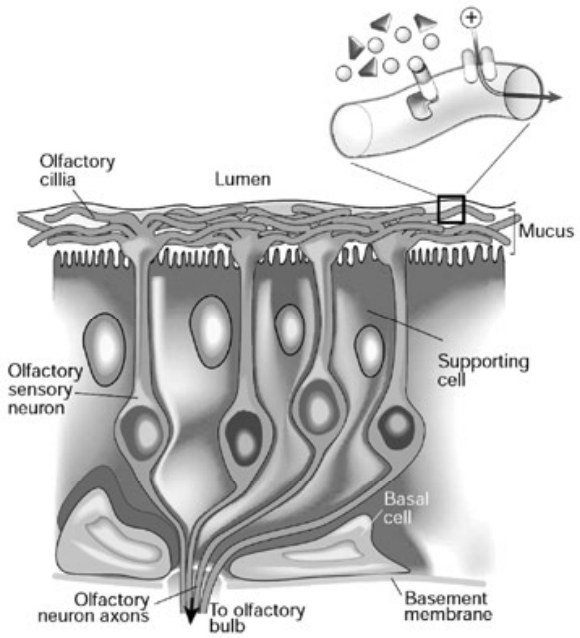

Figure 4. Cross section of olfactory epithelium. OSNs are located within the OE along with supporting (or sustenacular) cells and basal cells. Basal cells give rise through asymmetric division to new OSNs. Turnover of OSNs occurs throughout the lifespan of the organism. From the tip of their apical dendritic knob, OSNs extend numerous cilia into the mucous covering the OE within the nasal cavity, where they encounter odorants. At the proximal end, OSNs extend axons that travel to the OB.

dendrite terminates in a rounded structure called a dendritic knob on the surface of which there are up to ten cilia. These cilia express ORs at their surface and extend into the mucus lining the surface of the nasal epithelium. Odorants dissolved in the mucus or, in the case of non-water soluble odorants, bound with odorant binding proteins bind to the ORs thus initiating odorant signal transduction.

From the basal pole of the OSN, a long, thin, unbranched axon passes through perforations in the bony cribiform plate at the base of the skull. OSNs enter the OB, forming its outermost layer, the olfactory nerve layer (ONL). They then pass into a layer called the glomerular layer (GL), made up of discrete tangles of neuropil called glomeruli. Each OSN targets one glomerulus wherein it branches (Hálasz and Greer, 1993; Klenoff and Greer, 1998), synapsing with both central output and interneurons.

As already mentioned, OSNs appear to be predominantly morphologically homogenous. However, they exhibit dramatic molecular heterogeneity, most notably due to the fact that each OSN is thought to express only one of the 1,000 ORs encoded in the genome (for discussion see Mombaerts, 2004). Furthermore, each OSN expresses only one of the two (maternal and paternal) alleles of a given OR, thus resulting in approximately 2000 subpopulations of OSNs (Mombaerts, 2006). The mechanisms that regulate gene choice in the OSNs are not presently known, but the OSN nevertheless offers an attractive model for studying the molecular biology of gene expression/choice.

OLFACTORY GLOMERULUS

OSNs expressing different ORs appear to be randomly distributed throughout multiple overlapping bands in the OE (Iwema *et al.*, 2004, Miyamichi *et al.*, 2005). On the other

hand, it is generally accepted that all OSNs targeting a given glomerulus express the same OR (Treloar et al., 2002), although heterogeneously innervated glomeruli do appear transiently in the developing OB (Zou *et al.*, 2004). This is a remarkable feat of reorganization, given that OSN axons are originally arranged in fascicles reflecting their point of origin in the OE. The sorting of axons containing the same OR occurs within the ONL (Treloar *et al.*, 2002).

The mechanisms whereby OSN axons expressing one OR converge on a specific glomerulus have not yet been fully elucidated (for a thorough review, see Mombaerts, 2006). It is clear, that ORs themselves participate in the glomerular specificity of targeting (Mombaerts *et al.*, 1996), though they alone are not sufficient for correct OSN targeting (Wang *et al.*, 1998). In addition, multiple other molecules such as OCAM (Treloar *et al.*, 2003) or cell surface carbohydrates (Lipscomb *et al.*, 2003; for review see Treloar *et al.*, 2002) as well as functional activity (Lin *et al.*, 2000; Zheng *et al.*, 2000) likely play a role.

The glomerulus is an anatomically defined processing module, analogous in some respects to the anatomical organization of visual input seen with ocular dominance columns in the visual cortex. It is an ovoid or circular structure encircled by glial cells as well as a variety of intrinsic neurons such as PG, juxtaglomerular and short-axon cells (Shepherd *et al.*, 2004). In rodents glomeruli range in size from 30-50μm in the mouse to around 100μm in the rat, although microglomeruli have been described (Lipscomb *et al.*, 2002).

Each glomerulus is innervated by several thousand OSNs (Allison, 1953) and there are a total of approximately 1600-1800 glomeruli in the mouse OB (Royet, 1988).

As discussed above, each glomerulus is molecularly homogenous insofar as it receives input representing a single OR. Furthermore, OSNs expressing a given OR appear to innervate two glomeruli per bulb, one medial and one lateral, resulting in a total of four glomeruli per animal registering a given OR signal. Based on work in the hamster, Schoenfeld and his colleagues (1985) identified an intrabulbar association network that links the medial and lateral glomeruli receiving input from the same subpopulation of OSNs via TC axon collaterals.

This organization allows for spatial coding of the identity and concentration of an odorant. Numerous studies have shown stereotyped glomerular array activation in response to a given odor stimulus using 2-deoxyglucose mapping (Stewart *et al.*, 1979; Jourdan *et al.*, 1980; Greer *et al.*, 1982), using c-*fos* (Guthrie *et al.*, 1993) and fMRI (Yang *et al.*, 1998). Recent work has also begun to elucidate a temporal glomerular code component (for a complete review of odor information coding at the glomerular level see Wachowiak and Shipley, 2006; Leon and Johnson, 2003).

A finer level of organization has also been described within individual glomeruli, further complicating the emerging picture of the spatial component of odor encoding. Features of compartmental organization that have been identified include non-random ramification of OSN axon termini within glomeruli (Hálasz and Greer, 1993), segregation of OSN axons from MC dendrites (Kasowski *et al.*, 1999; Kim and Greer, 2000) and heterogeneous distribution of synapses (Johnson *et al.*, 1996). Walz and his colleagues (Walz et al., 2006) have shown that while OSN targeting to individual glomeruli is maintained, glomerular compartmental organization is disrupted in knockout mice lacking the olfactory cellular adhesion molecule, OCAM.

MITRAL CELLS

Mitral cells are the principal projection neuron in the OB. In the adult, MCs are known to exhibit a highly stereotyped morphology. The somata, from which MCs draw their name due to their resemblance to a cardinal's mitre hat in cross section, are 15-30µm in diameter. The cell body gives off a single apical or primary dendrite that can be 200µm to 800µm long. The primary dendrite extends towards the surface of the OB and terminates in a glomerulus in a profuse dendritic tuft known as a dendritic or glomerular tuft. The glomerular tuft has a diameter of 15-30µm (Shepherd *et al.*, 2004). This tuft is the site of axodendritic connections with afferent OSNs as well as dendrodendritic (bi-directional) synapses with PGs.

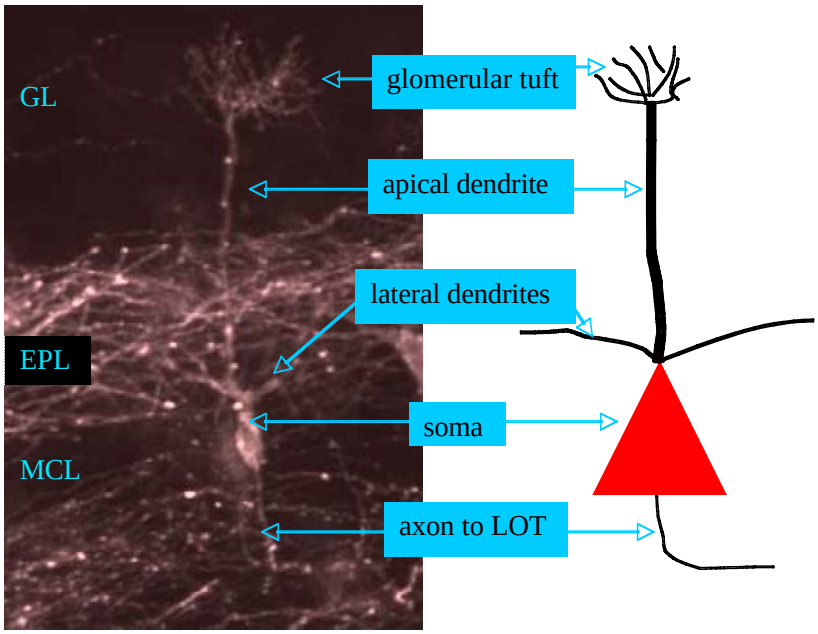

Figure 5. Mature MC morphology. DiI labeled MC from P10 mouse and schematic drawing of an adult MC, demonstrating the stereotypic adult morphology including (from distal to proximal): the glomerular tuft at the end of a single, apical dendrite, several lateral dendrites, the mitre-shaped soma and an axon.

In addition, the adult MC exhibits lateral or secondary dendrites that run parallel to the surface of the OB through the EPL for anywhere from 500µm to over 1000µm (Greer, 1987; Mori *et al.*, 1983; Shepherd *et al.*, 2004). A hallmark of the OB circuitry occurs in the external plexiform layer where the MC secondary/lateral dendrites establish

reciprocal dendrodendritic synapses with granule cells (interestingly, these were the first dendrodendritic synapses identified in the nervous system). These are thought to provide for both feedback- as well as lateral-inhibition (Chen *et al.*, 1997; Isaacson and Strowbridge, 1998; Schoppa *et al.*, 1998).

At the basal pole the MC extends a single axon, which runs deep and caudally to the posterolateral OB where it fasciculates with other axons to form the lateral olfactory tract (LOT). MC axons also give off recurrent collaterals, as previously touched upon, within the IPL and the GCL as well as numerous collaterals in the LOT.

Approximately 25 MCs are thought to innervate one glomerulus (Shepherd *et al.*, 2004). Given that several thousand OSNs innervate a single glomerulus, this represents a convergence ratio on the order of 1:1000. Evidence suggests that MCs innervating the same glomerulus are neighbors within the MCL (Bounviso *et al.*, 1991; Zou *et al.*, 2001). There have been numerous attempts to elucidate a functional organization to the MC layer, but so far these have been inconclusive. For instance, Buonviso and Chaput (1990) recorded individual MCs with micropipettes placed no more than 40μm apart and found that 95% of cell pairs exhibited similar response patterns to given odor stimuli. However, more recent studies (e.g., Nagayama *et al.*, 2004) have observed differing responses to odorants in MCs located in the same cluster.

It is important to note that the present research focuses its attention on MCs. Although there is a second population of projection neurons, the TCs, limiting our inquiry was necessary to allow thorough examination of the subject. Furthermore, MCs and TCs are sufficiently distinct as to make the limitation in scope justified.

DENDRITIC DEVELOPMENT

Our understanding of mechanisms that influence dendritic development and targeting in the central nervous system lags significantly behind our understanding of the mechanisms that influence axonal targeting. Indeed, it is only the past few years that have seen any attention given to the question of dendritic targeting in the nervous system (for review see Keith and Wilson, 2001). Historically, based largely on studies of the visual system, it has been thought that dendrites tended to innervate broadly and diffusely and that specificity of connections emerged only with coordinated functional/axonal input. More recently, it has been recognized that even during early development, dendrites begin to exhibit the targeting specificity that will be their phenotypic hallmark following maturation (e.g. Gao *et al.*, 1999). Furthermore, it appears that many of the same molecular cues involved in axonal and dendritic guidance and targeting (for review see Kim and Chiba, 2004)

The precision with which dendrites arborize and innervate specific laminae in the adult brain is striking. For example, pyramidal neurons in the hippocampus and throughout cortex extend apical and basal dendrites that organize into highly stereotyped patterns that appear relatively invariant. While the earliest appearance of these arbors lacks the extreme precision seen in the mature animal, at even the youngest ages specificity is recognized (Crowley and Katz, 2000).

The emerging consensus is that while functional activity may contribute to the fine-tuning of cortical maps, molecular protomaps must initially define organization (for review see Cline, 2001). Clear evidence of this is seen with the Ephs/Ephrins, which delineate regions of occipital cortex prior to the arrival of sensory axons from the

thalamus (Sestan *et al.*, 2001). Further support comes from the recent finding that Semaphorin 3A, in conjunction with its receptor Neuropilin-1, can act as a tropic agent directing the growth of cortical pyramidal neurons toward the pial surface (Polleux *et al.*, 2000). Other candidate ligand–receptor pairs whose roles in dendritic guidance have been explored in the invertebrate system are Netrin–Frazzled (Furrer *et al*., 2003) and Slit– Robo (Whitford *et al*., 2002).

MITRAL CELL MATURATION AND DENDRITIC DIFFERENTIATION

The mechanisms that underlie the differentiation, maturation and targeting of MC apical dendrites for one versus another glomerulus have not yet been fully elucidated.

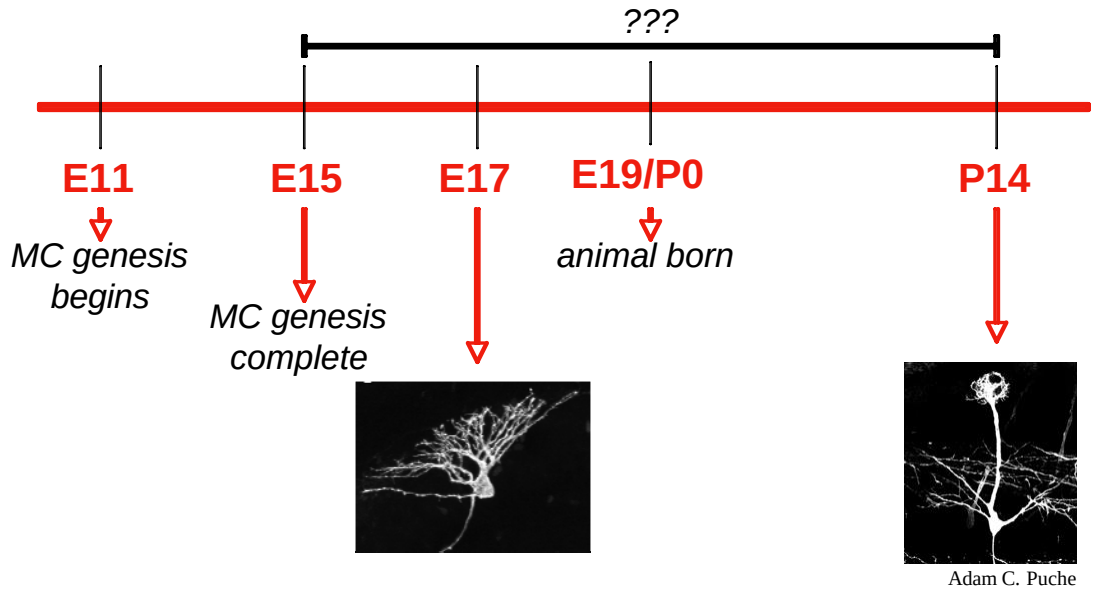

Figure 6. Characterizing spatiotemporal pattern of MC dendritic development. By E15 MC genesis is complete (Hinds & Ruffett, 1973). At E17 MCs exhibit multiple supernumerary dendrites in a broadly spread dendritic arbor. The animal is born on the 19th day of gestation. By the 14th postnatal day (P14) MCs have achieved the characteristic adult MC morphology including a singly apical dendrite that extends perpendicular to the surface of the OB, terminating in a glomerular tuft in the GL and several secondary dendrites extending parallel to the surface of the bulb within the EPL (our observation). The focus of the present research is characterizing the transitional stages between E15, when MCs have all been born and P14 the outermost day, when we can safely observe that MC have adopted their mature dendritic morphology.

Malun and Brunjes (1996) showed in the opossum, and to a lesser extent in the rat, that mitral cells in the main OB initially have supernumerary processes that are broadly spread across the presumptive glomerular layer, extending up to approximately 100 µm at birth while in the adult the spread appears limited to about 50 µm within a single glomerulus. However, mitral cell maturation and dendritic differentiation have not been definitively characterized in the mouse, the current model system of choice.

López-Mascaraque and her colleagues (1998) observed the formation of an OB-like structure with MC-like cells in homozygous *Pax-6* mutant mice, in whom OE never develops and afferent activity does not reach the OB. However, although OB- and MC-like structures were present, the group showed that MC dendrites are not properly oriented towards the GL at the surface of the OB (López-Mascaraque *et al*., 2005). This evidence suggests that these events are not purely intrinsic or cell-independent and that input from the OSNs, or perhaps even centrifugal inputs, may modulate or contribute to the differentiation and targeting of dendrites.

Although multiple factors are currently being explored as possible contributors to dendritic maturation and targeting, an important area of research has been the role of functional activity, based on its role in the dendritic development in other systems (for review see Wong and Ghosh, 2002). There have been several studies suggesting significant interruption of MC development as a result of sensory deprivation. For example, two separate studies, Meisami and Noushinfar (1986) via naris-occlusion and Couper Leo and Brunjes (2002) by means of focal denervation, show significant reductions in the size of both apical and secondary MC dendritic arbors following sensory deprivation. Matsutani and Yamamoto (2000) observed delays in MC

maturation and perturbation of secondary dendrite development in the rat in response to neonatal naris-occlusion. Furthermore, there is evidence of decreases in somatodendritic synapses between MCs and GCs in the absence of functional activity (Benson *et al.*, 1984).

On the other hand, Lin *et al.* (2000) suggested that the trimming of supernumerary processes to only one apical dendrite arborizing in a single glomerulus is independent of functional activity. They reported that apical dendritic trimming occurs in mice in which the alpha subunit of the cyclic nucleotide channel is knocked out, resulting in a loss of odor-induced activity in OSNs. Because MC dendritic differentiation appeared to occur without aberrations, these data suggest that mechanisms other than functional afferent input may influence the targeting of glomeruli by mitral cell apical dendrites. However, the Lin et al. (2000) study does not address the effects of spontaneous activity in the absence of odor induced activity or, the possibility of biochemical gradients induced by odorant binding to ORs. Thus, the problem remains controversial.

Consistent with the notion that targeting of glomeruli may be under the control of mechanisms independent of functional activity is the organization of the accessory OB. In contrast to the main OB, the apical dendrites of mitral cells in the accessory OB innervate more than one glomerulus (Takami and Graziadei, 1991). In parallel, the axons of the vomeronasal sensory neurons do not coalesce to terminate in only 2 or a few glomeruli as occurs in the main OB but rather, distribute broadly and in complex patterns in the glomerular layer of the accessory OB (Rodriguez *et al.*, 1999). A similar organization is found in the zebrafish OB where mitral cells have multiple apical dendrites that innervate multiple glomeruli (Yoshihara and Mori, 2001). These

multiglomerular arborization patterns for both sensory axons and dendrites make it difficult to conceive of how coordinated functional activity could be a pivotal requirement for targeting in these systems.

Statement of Purpose

It is clearly essential that for interpretable neuronal signaling to occur, the targeting and arborization of MC dendrites must be correct. Not only is it necessary for the apical dendrites to correctly target a glomerulus but the secondary dendrites must also be appropriately distributed within the deeper sublamina of the external plexiform layer. To begin to assess the substrates of MC dendritic differentiation we have first sought to characterize the developmental stages in the mouse where future studies would benefit from the availability of molecular biological and genetic tools. Secondly, we have introduced a new reagent, a MC dendritic growth cone specific marker that has enabled us to address more directly the maturational events occurring within the external plexiform layer and its constituent sublaminae. We hypothesized that both lines of data will show evidence of significant postnatal dendritic remodeling.

METHODS

MITRAL CELL DENDRITIC DEVELOPMENT

Tissue preparation

Embryonic age mice were obtained from timed-pregnant CD-1 mothers (Charles River, Wilmington, MA) by caesarian section and immediately decapitated. Neonatal mice (Charles River Laboratories) were sacrificed by CO_2 inhalation and decapitated. Embryos and neonatal mice were drop-fixed in 4% paraformaldehyde (PFA) in 0.1M phosphate buffered saline (PBS; 0.9% saline) and kept in 4% PFA at 4^0C until used. Postnatal (P) mice (P6 and older, Charles River) were anaesthetized with 1ml nembutal (Abbott Laboratories, North Chicago, IL), transcardially perfused, first with PBS and then with 4% PFA in PBS. After the brain was dissected out, it was kept in 4% PFA in PBS at 4^0C until use.

DiI Labeling

MCs were retrogradely labeled with1,1'-dioctadecyl-3,3,3',3'-tetramethylindocarbocyanine perchlorate (DiI; Molecular Probes, Eugene, OR). DiI is a lipophilic molecule that diffuses in plasma membranes in fixed or living tissue. DiI was loaded into the lateral olfactory tract (LOT) using a minutien pin dipped in DiI crystals. The pin was inserted and immediately retracted, after which brains were replaced in 4% PFA in PBS and kept at room temperature (RT) for 4-14 days, in proportion to the age of the animal. Brains were blocked in 2% agarose in PBS, sectioned at 100-150µm on a Pelco 101 vibratome, mounted on precleaned slides (Esco, Portsmouth, NH) and cover-slipped (Fisherbrand Scientific, Pittsburgh, PA). Labeled MCs were imaged on an MRC-

600 laser confocal microscope or on a Leica TCS SL confocal microscope; Z-series were collected throughout the thickness of the cell at 0.2-1µm intervals.

SPATIOTEMPORAL PATTERN OF CDA 1 EXPRESSION IN THE OB

Tissue preparation

Brains were obtained as described above. Embryonic and neonatal brains were immersion-fixed in 4% PFA in PBS for a minimum of two hours and maximum overnight at 4^0C. Adult brains were also immersion-fixed for at least 2 hours or overnight at 4^0C after perfusion. Brains were then rinsed in PBS for 2 hours or overnight at 4^0C. They were immersed in 30% sucrose in PBS for cryo-protection until the tissue sank and then embedded in Tissue Teck O.C.T. compound (Sakura Finetek, Torrance, CA). The tissue was kept at -80^0C until sectioning. OB tissue was sectioned at 20µm using a cryostat (Reichert-Jung 2800 Frigocut E) and mounted on glass slides (Fisherbrand). Slides were kept at -20^0C until use.

Immunohistochemistry

Sections were first allowed to come to room temperature (RT). A border was painted onto the glass with silicone sealant (Permatex, Solon, OH). Sections were pre-incubated in 2% bovine serum albumin (BSA; Sigma) in Tris-buffered saline (TBS; 0.1M Tris buffer in 0.9% saline) with 0.3% Triton X-100 (TX; Sigma-Aldrich, Chemical Co., St. Louis, MO; TBST) for 30 minutes to block non-specific binding sites. Sections were then incubated with primary antibodies including mouse anti-CDA 1 IgG antibody (undiluted ascites fluid, gift of Dr. Colin J. Barnstable, (Devoto and Barnstable, 1989)) and chicken anti-MAP-2 antibody (1:1000, Chemicon, Temcula, CA), washed 3 times in

TBST and then incubated with secondary antibodies. Secondary antibodies included Alex-488-conjugated goat-anti mouse IgG and Alexa-568-conjugated goat-anti chicken antibody (1:1000, Molecular Probes). Sections were washed again in TBST 3 times, then rinsed with TBS once and cover-slipped with Gel/Mount mounting medium with anti0fading agents (Biomeda, Foster City, CA). Sections were stored in the dark at 4^0C until use.

Tissue Culture

OB enriched neuronal cultures were prepared from PO pups. At P0 the majority of cells are mitral or tufted cells, with few granule or interglomerular cells present (Hinds, 1972a,b). Heads were harvested as described above and dropped in Hank's balanced salt solution without calcium or magnesium (HBSS, Gibco BRL, Invitrogen Corp., Carlsbad, CA). After they were dissected out and the meninges removed, OBs were minced. Treatment with 0.25% trypsin solution (Sigma) for 30 minutes was used to dissociate cells. Dissociated cells were then treated with 0.02% trypsin inhibitor (Sigma), rinsed 3 times in HBSS with calcium and magnesium (HBSS+, Gibco BRL), triturated in Neurobasal medium supplemented with B27, 0.5mM L-glutamine, and 1% penicillin/streptomycin (all from Gibco BRL). Cells were then plated on poly-D-lysine-coated (1µg/ml, 30-70 kDa, Sigma) cover glass (22mm^2, VWR Scientific, Media, PA) at a cell density of $6x10^3$ cells/cm^2. Cells were maintained in a humidified incubator at 37^oC and 5% $C0_2$ and fed with supplemented Neurobasal medium every 2-3 days for a minimum of 14 days. This culturing technique has been applied previously in the Greer lab and is optimized to promote neuronal growth and to suppress glial growth. The cultures were fixed in 4% PFA and 4% sucrose in PBS for 30 minutes, then rinsed with

PBS. Cells were permeabalized with 0.3% Triton X-100 (Sigma) for 5 minutes, rinsed with PBS, the pre-incubated with 10% BSA in PBS for 20 minutes to block nonspecific binding sites. Cells were incubated in primary antibodies: mouse anti-CDA 1 (undiluted ascites fluid), mouse anti-β tubulin III IgG2b (1:200, Sigma) and rabbit anti-glutamine (1:200, Sigma) for 1 hour, washed 3 times with PBS, then with secondary antibodies diluted in blocking solution for 30 minutes. Secondary antibodies included and Alex-568-conjugated goat-anti mouse IgG antibody (1:1000; Molecular Probes) and an Alexa-488-conjugated goat-anti rabbit antibody (1:1000, Molecular Probes). Sections were washed in PBS 3 times and mounted in Prolong mounting medium (Molecular Probes), cover-slipped, and imaged using the Bio-Rad MRC-600 laser scanning confocal microscope.

Microscopy

For quantitative data analysis, images were collected with an Olympus MagnaFire digital camera mounted on an Olympus BX51 upright microscope. For qualitative data, images were collected at 40X, and oil-immersion 60X using an MRC-600 laser confocal microscope or on a Leica TCS SL confocal microscope (P0, n=4; P4, n=5; P8, n=2). Figures were designed using CorelDraw 10 (Corel, Ontario, Canada).

Data Analysis

Image analyses for quantitative assessment of CDA 1 expression *in vivo* was accomplished using ImageJ (freeware, NIH). Regions of interest (ROI) were outlined on merged images of CDA 1 and MAP-2 immunostaining, using MAP-2 staining to help delineate the lamina. Images were split and the CDA 1 black and white image was thresholded to exclude all backround staining within the ONL and the total CDA 1 positive area within the ROI was measured. Comparisons were made using the ratio of

total CDA 1 positive are to total ROI area. Statistical analyses were performed using GraphPad Prism, version 4 (GraphPad Software Inc., Sand Diego, CA).

CONTRIBUTIONS

I performed all of the DiI injections, immunohistochemistry, tissue sectioning, imaging and data analysis. I am indebted to Dr. Helen B. Treloar for providing me with cell cultures for in vitro examination of CDA 1 expression and to Dolores Montoya for assistance with animal sacrifice, perfusion and tissue preparation.

RESULTS

MC DENDRITIC DEVELOPMENT USING DiI FILLS

The first goal of this project was to extend our understanding of the morphological patterns/stages of MC dendritic development in mice (Malun and Brunjes, 1996; Matsutani and Yamamoto, 2000). Using DiI injections into the lateral olfactory tract in order to retrogradely label MC bodies and dendrites, we examined the

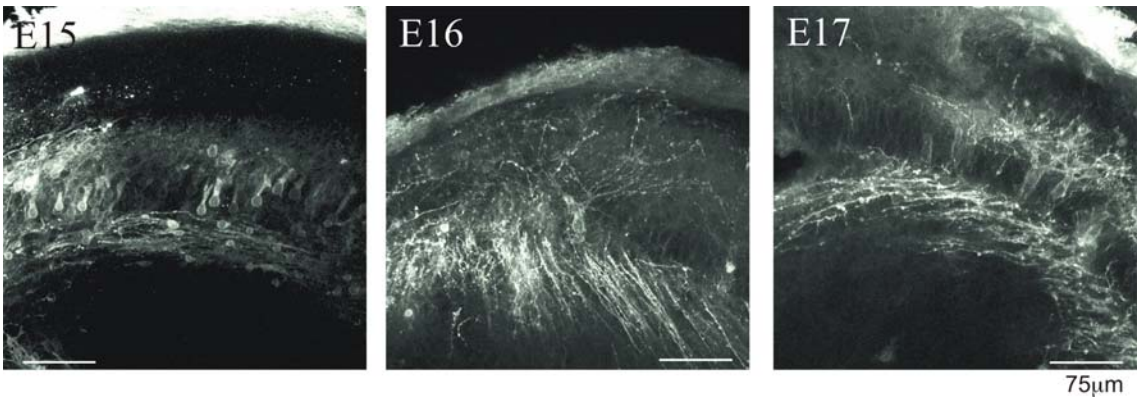

Figure 7. Embryonic MC dendritic development. MC dendrites retrogradely labeled with DiI. At E15, the somata of MCs exhibit a leading dendritic process almost as wide as the cell body itself. By E16, most MCs appear to exhibit more complex dendritic morphology with a diffuse dendritic arbor of approximately uniform dendritic processes. By E17, MCs demonstrate a dendritic arbor with supernumerary dendrites.

morphology of MC dendritic arborization in the mouse main OB at embryonic ages E15 through E17 (figure 7) and postnatal ages from P0 to P10 (figure 8).

MCs progressed through a wide spectrum of dendritic morphologies in this age range. At E15, MCs exhibited a simple morphology consisting of a cell body with a leading dendritic process almost as wide as the cell body itself, which appears to be in a spectrum of orientation with respect to the surface of the OB from parallel to perpendicular. By E16, most MCs appeared to exhibit more complex dendritic morphology with a diffuse dendritic arbor of approximately uniform dendritic processes.

By E17, all MCs acquired a dendritic arbor with supernumerary dendrites that appeared to be broader than at earlier ages.

At P0 MCs continue to exhibit this immature morphology, projecting supernumerary, undifferentiated dendrites at various angles broadly throughout the EPL

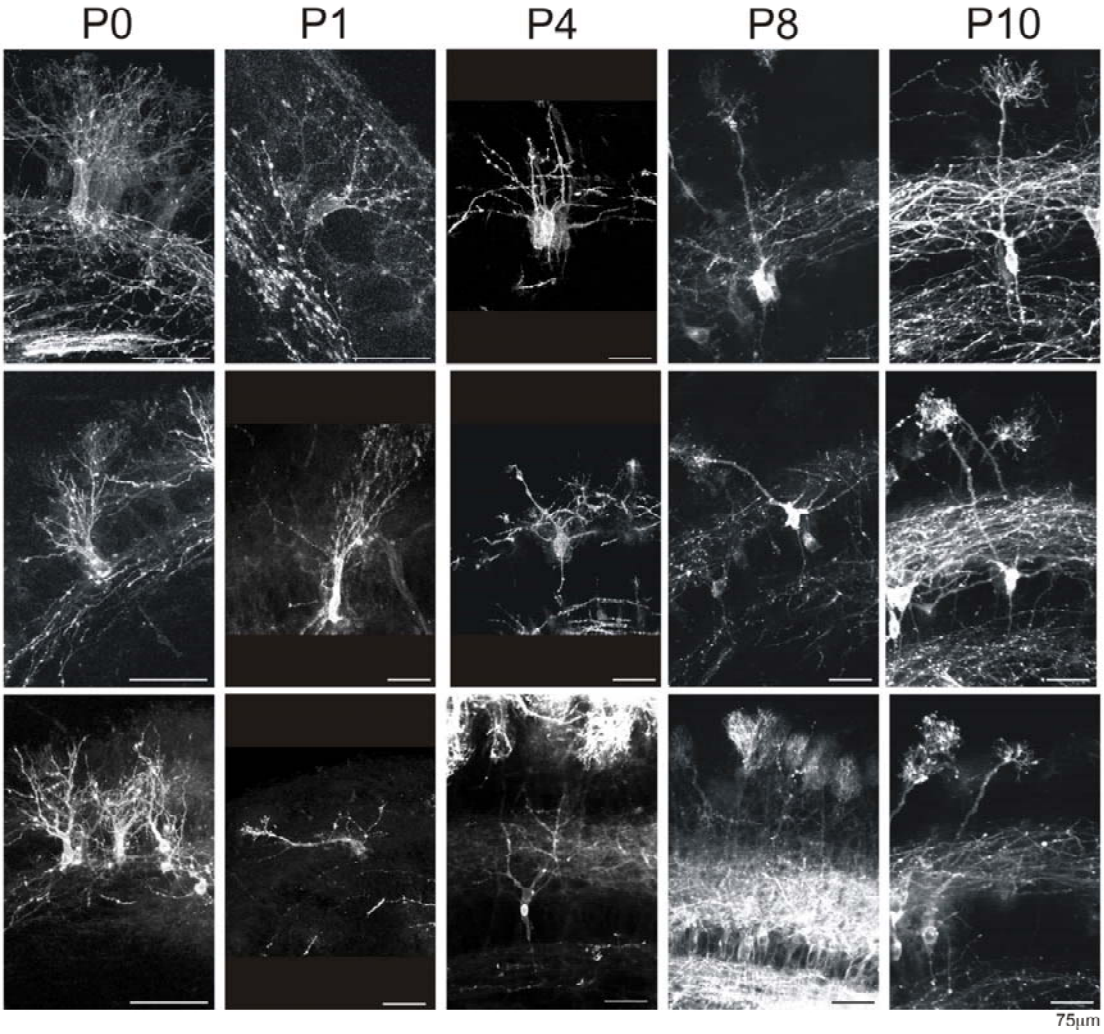

Figure 8. Postnatal MC dendritic development. Representative postnatal MCs retrogradely labeled with DiI at four ages, P0, P1, P4, P8, P10. At P0 MCs exhibit supernumerary, undifferentiated dendrites broadly projecting throughout the EPL. There appears some variation in the morphologies at P0, with some cells exhibiting preferential thickening of some of their dendrites. At P1, the MC dendritic arbor narrows and one dendrite appears thicker than the others, likely the proto-apical dendrite. At P4, the MC dendritic arbor narrows further and consists of two subsets of dendrites: a primary, thicker dendrite projecting straight into the EPL perpendicular to the surface of the OB. In addition, at P4 MCs have a variable number of secondary, thinner dendrites, that project laterally within the EPL, parallel to the surface of the OB. By P8, the mature adult dendritic morphology emerges, including one primary apical dendrite that projects radially into the EPL, ending in a glomerular tuft extending perpendicular and into the EPL as well as several thinner secondary dendrites extending parallel to and within the EPL. This dendritic morphology persists at P10.

and toward the nerve layer of the OB. However, by P0 there appears to be some variation in the morphologies as some cells did exhibit preferential thickening of some of their dendrites. By P1, the MC dendritic arbor does not appear as broadly spread, perhaps reflecting pruning of some of the supernumerary dendrites, and one dendrite appears thicker than the others, perhaps the proto-apical dendrite, although at this age, the dendritic arbor continues to project broadly, at various angles with respect to the surface of the OB, throughout the EPL. By P4, the MC dendritic arbor narrows further. Although supernumerary dendrites still occur, the dendritic arbor at P4 consists of two clearly apparent subsets of dendrites: a primary, thicker dendrite projecting radially into the EPL, perpendicular to the surface of the OB and a variable number of secondary, thinner dendrites, projecting laterally within the EPL, parallel to the surface of the OB. By P8, we observed the emergence of a mature adult MC dendritic morphology, as previously characterized in the opossum by Malun and Brunjes (1996), including one primary apical dendrite ending in a glomerular tuft extending perpendicular and radially into the EPL as well as several thinner secondary dendrites extending parallel to and within the EPL. This mature adult MC dendritic morphology persists at P10 and indeed throughout adulthood. Interestingly, there was greater variation in stages of maturation of MC dendritic morphology at any given age than we had hypothesized.

CDA 1 EXPRESSION IN THE OB

Our DiI analyses qualitatively characterized MC dendritic development in the mouse OB from an immature dendritic arbor consisting of broadly spread, uniform supernumerary dendrites to the mature MC dendritic morphology, including a single

apical dendrite ending in a glomerular tuft and several secondary dendrites extending laterally in the EPL. However, we needed a quantitative approach that would provide a reliable index of dendritic remodeling within the EPL; further, we wanted to assess if spatiotemporal patterning occurred within the EPL during development. To meet these needs we used CDA 1, a growth cone specific antibody, as a marker for time course and spatial distribution of developing dendrites. Growth cones are found at the leading edges of growing axons and dendrites and their presence may thus be used as a relative index of neurite extension and active growth.

CDA 1 is an epitope on an intracellular molecule that localizes to neuronal growth cones, first described by Devoto and Barnstable (1989) in the rat. While the prior report focused on the cerebral hemispheres, they noted CDA 1 expression in the olfactory bulbs as well. Taking advantage of this observation, we hypothesized that the patterns of expression exhibited by CDA 1 could be used to identify dendritic developmental waves that can be described by laminar patterns.

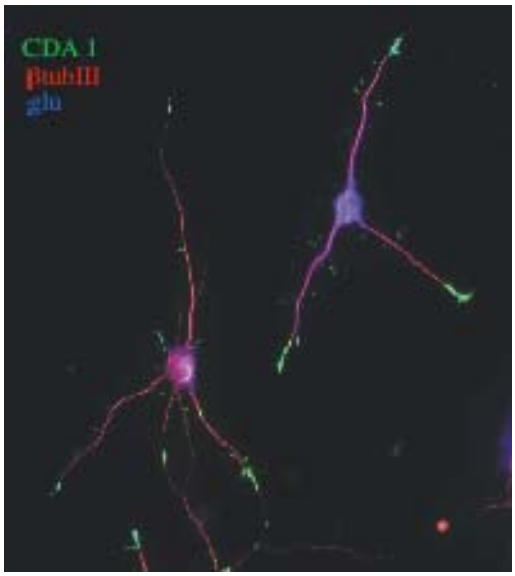

Figure 9. CDA 1 is expressed in MC growth cones *in vitro*. Cultured MCs immunostained with β-tubulinIII, glutamate, and CDA 1. Mitral cells are identifiable by their characteristic mitre-shaped cell bodies. In addition, since MCs are glutamatergic, they are glutamate antibody immunoreactive. CDA 1 occurs most densly at the leading edges of MC neurites in a growth cone-like pattern.

To verify the specificity of CDA 1 labeling of MC dendritic growth cones, we first looked *in vitro* expression of CDA 1 by MCs in primary OB culture. To identify MCs and determine co-localization with CDA 1, we triple labeled using anti-CDA 1

antibody, anti-glutamate antibody and anti-β tubulin III antibody, a neuronal marker (figure 9). Using a culture protocol previously designed and utilized in the Greer lab to enhance the presence of MCs relative to other OB cell types, MCs were easily identified morphologically, based on their distinct, large, mitre shaped somata. Because MCs are glutamatergic neurons, immunoreactivity with anti-glutamate antibody further confirmed MC identity (Shepherd *et al.*, 2004). CDA 1 immunoreactivity appeared as ovoid staining at the tips of neurites. We found that CDA 1 expression is restricted to undifferentiated neurites and nascent dendrites, exhibiting a characteristic growth cone-like appearance at the tips of extending processes. Labeling with CDA 1 was not found in the cell body or in the shafts of extending neuritis/processes. Moreover, CDA 1 did not stain the nascent MC axon growth cone, providing further evidence for the dendritic growth cone specificity of the antibody.

Having established CDA 1 specificity for developing MC neurites/dendrites *in vitro*, we proceeded to examine CDA 1 expression in whole olfactory bulb frozen sections. *In vivo*, CDA 1 immunoreactivity appeared as scattered punctate staining, with each individual CDA 1 positive point ranging from 3-8μm along the long axis and approximately 3μm along the short axis (figure 9). We observed CDA 1 expression in both the EPL and the GL, areas rich in developing dendrites. We did not observe CDA 1 staining in the ONL, which is clearly delineated as the outermost, MAP-2-free lamina, indicating the absence of dendrites. Because the ONL is a region of robust and ongoing axon extension, with a commensurate high density of axonal growth cones, the absence of staining in the ONL is further support for our interpretation that CDA 1 is dendrite specific.

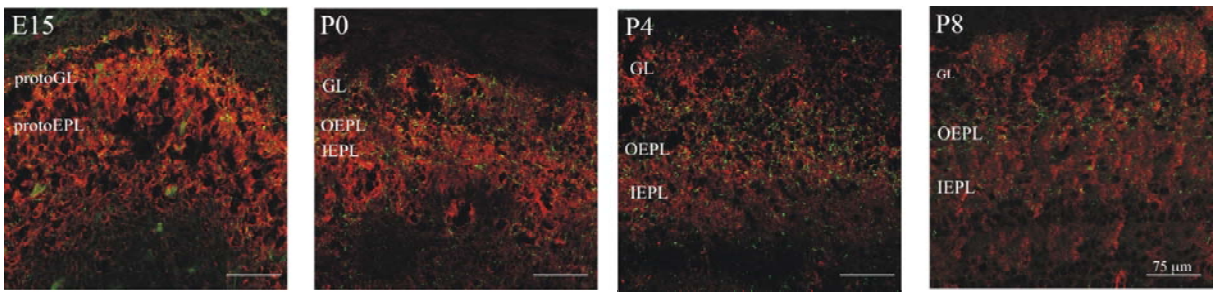

Figure 10. CDA 1 is expressed with laminar and sublaminar specificity *in vivo*. Mouse OB cross sections immunostained with CDA 1 and MAP-2. CDA 1 is apparent as punctate green staining dispersed throughout the the EPL and the GL, areas rich in developing dendrites. CDA 1 is not present in the ONL, clearly delineated as the outermost, MAP2-free lamina, indicating the absence of dendrites.

CDA 1 expression exhibits inter- and intralaminar patterns of development in the olfactory bulb (figure 10). We focused our attention on the EPL and GL, where MC dendrites ultimately take up position. In both the EPL and GL we observed an overall downward trend from P0 to P8. By P21, CDA 1 expression has decreased to undetectable or insignificant levels (personal observations).

Furthermore, as there seemed to be intralaminar differences in CDA 1 expression patterns in the EPL, we decided to divide the EPL into an inner (iEPL, deep 1/3) and outer (oEPL, superficial 1/3) layer for separate analyses of CDA 1 expression. This subdivision yielded a significant difference between CDA 1 levels in iEPL vs. oEPL (P0, $p<0.001$, n=4; P2, $p<0.001$, n=4; P4, $p<0.001$, n=3; P8, $p<0.05$, n=3), corroborating the previous observation and justifying the decision of sub-diving the EPL into two sublaminae.

In the iEPL, CDA 1 levels decrease significantly between P0 and P2 (n=4, P0vsP2, $p<0.001$; 1way ANOVA with Tukey's Multiple Comparison post-Test). In the oEPL, CDA 1 expression is relatively constant throughout PO to P4 (P0vsP2, $p>0.05$, P0vsP4, $p>0.05$, P2vsP4, $p>0.05$; 1way ANOVA with Tukey's Multiple Comparison post-Test). CDA 1 expression is then downregulated in the oEPL between P4 and P8

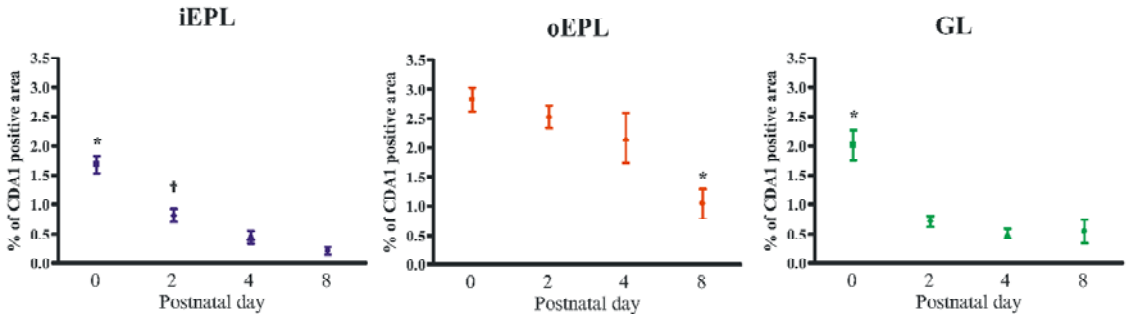

Figure 11. CDA 1 expression in the OB exhibits laminar and sublaminar developmental patterns of expression. CDA 1 expression within OB laminae at P0, P2, P4, and P8. In the iEPL, CDA 1 levels decrease significantly between P0, P2 & P4 (P0vsP2, $p<0.001$). The oEPL exhibits no significant change in CDA 1 expression from P0 to P4 and then down regulates between P4 & P8 (P4vsP8, $p<0.05$). Furthermore, highest levels of CDA 1 are achieved in the oEPL. In the GL, CDA 1 levels decrease significantly from P0 to P2 (P0vsP2, $p<0.001$) and then are stable through P8.

(P0vsP8, $p<0.001$, P2vsP8, $p<0.01$, P4vsP8, $p<0.05$; 1way ANOVA with Tukey's Multiple Comparison post-Test). Furthermore, we observed higher levels of CDA 1 expression in the oEPL than in the iEPL throughout the ages we examined. In the GL, there is a significant decrease in CDA 1 levels between P0 and P2 (P0 vs. P2, $p<0.001$, P0 vs. P4, $p<0.001$, P0 vs. P8, $p<0.001$, 1way ANOVA with Tukey's Multiple Comparison post-Test), after which they appear stable through P8 (P2 vs. P4, $p>0.05$, P2 vs. P8, $p>0.05$, P4 vs. P8, $p>0.05$ 1way ANOVA with Tukey's Multiple Comparison post-Test).

In addition, we have made preliminary observations suggesting that there is a pattern to the dendritic development along the rostrocaudal axis (figure 12). Collapsing the data from the iEPL, oEPL, and GL for each of 3 ages, P0, P4, and P8, we noted that there appears to be a temporal wave of CDA 1 expression along the rostrocaudal axis. It appears that CDA 1 expression is highest in the mid-OB at P0, highest in the rostral OB at P4 and in the caudal OB at P8. In addition, we again noted the overall downwards trend of CDA 1 expression from P0 to P8. This pattern suggests the possibility that

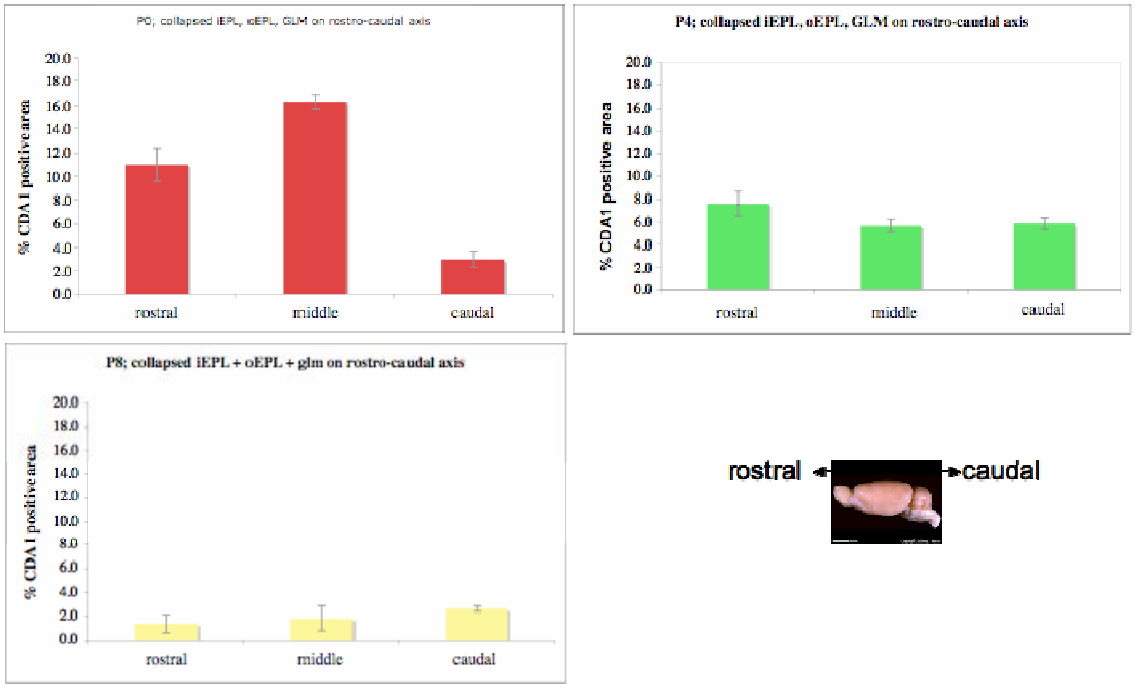

Figure 12. CDA 1 expression along rostrocaudal axis of OB. We have Our preliminary data suggests that CDA 1 expression may be variable along the rostro-caudal axis suggesting the possiblity of a rostro-caudal spatiotemporal wave of dendritic development. Above we have combined the analyses from the iEPL, oEPL, and GL at each of 3 ages and compared CDA 1 expression levels between these ages. The data suggests that CDA 1 expression is strongest in the mid-OB at P0, in the rostral OB at P4, and perhaps in the caudal OB at P8. In addition an overall decreasing trend in CDA 1 expression emerges, consistent with our previous results. Overall, this suggests a centripetal pattern of dendritic development.

dendritic development occurs in a centripetal wave from the mid OB towards the rostral and caudal poles.

DISCUSSION

The process whereby an undifferentiated neuroblast takes on the polarized morphology, including axons and dendrites exhibited by most adult neurons, is a vitally important component of the overall process of CNS development and communication. The MC is one such population of neurons exhibiting a highly stereotyped adult form that is essential for its proper functioning and connectivity. In the adult, it is known to consist of a pyramidal-shaped cell body, a long thin axon at the basal pole of the cell body and a single apical dendrite, which ends in a dendritic tuft in the glomerulus as well as several lateral dendrites extending through the EPL (Shepherd *et al*., 2004).

In a series of early studies looking at early neuron development in the mouse OB, Hinds (1972, 1973) made the observation that embryonic MCs exhibit supernumerary dendrites rendering them morphologically far different from the classic adult MC first described by Ramon y Cajal (1911). Subsequently, Malun and Brunjes (1996) used **r**etrograde DiI labeling of MCs in the opossum and, on a more limited scale, in the rat to look at MC dendrogenesis. However, in recent years the mouse has emerged as the dominant model system in the neurosciences, and specifically in the study of the molecular determinants of dendritic development and of the neural circuits involved in olfaction. Thus, we undertook a precise characterization in the mouse of the highly stereotyped and complex dendritic morphology of MCs, the projection neurons of the OB.

MCs genesis first begins as early as E11 and a defined MCL is first established at E15 (Hinds, 1972a,b; Hinds, 1973). The aim of this study was to begin to characterize

the timeline and sequence of MC dendrogenesis. We labeled MC dendrites in the mouse both embryonically, at E15 to E17, and postnatally from P0 to P10.

Our data indicate significant embryonic and postnatal, morphological changes in MC dendritic arbors. At E15, most MCs exhibit a leading, dendritic process that appears to be almost as thick as the soma, what Hinds (1973) termed a "perikaryon-dendrite." This makes sense, considering that MCs are still migrating into the OB and have not yet taken up position in the MCL, which is only beginning to emerge at E15 (Hinds, 1972a,b). By E17, however, the dendritic arbor appears to have broadened, acquiring a morphology similar to that seen on many MCs at P0 and corresponding well with the emergence of protoglomeruli at this age (Treloar *et al*., 1999).

At P0, when an animal is first exposed to air-borne odor stimuli, the dendritic arbor is broadly spread without the single glomerular specificity evident at later ages. Furthermore, variability is evident insofar as some cells appear to exhibit thickening of several of their dendrites while the dendrites are still of a relatively uniform thickness in others. The dendritic arbor then proceeds through a spectrum of intermediate morphologies. At P1, only one of the multiple, undifferentiated MC dendrites is thickened, presumably on its way to becoming an apical dendrite. At P4, many MC dendrites have more than one apical dendrite with multiple lateral dendrites. By P10, in a single MC one apical dendrite targets a single glomerulus while multiple lateral dendrites extend horizontally in the EPL.

Of some significance, OSN axons that target a single glomerulus all express the same odor receptor in the adult (Vassar *et al*., 1994; Treloar *et al*., 2002). In view of this, one can postulate that specific molecularly defined functional activity contributes to the

postnatal development of the apical dendritic arbor. The role of functional activity is currently controversial, but there are several studies indicating significant perturbation of MC morphology as a result of sensory deprivation (e.g., Matsutani and Yamamoto, 2000) or in the absence of OSN innervation (López-Mascaraque *et al*., 2005). Because there is some broad variability in the emergence of mature glomeruli (Treloar *et al.*, 1999) one may further speculate that differences in the maturation of individual MC apical dendrites may reflect variability in the maturation and arrival of OSN axons at specific glomeruli. In particular, Zou *et al.* (2004), have shown in the mouse that a glomerulus may be innervated by OSNs expressing more than one OR occur early on in development but that these heterogeneous glomeruli disappear in the mature OB. They further demonstrated that sensory deprivation may lead to persistence of heterogeneous glomeruli in the adult OB. In view of this, we may speculate that functional activity could influence MC dendritic activity via interaction with a homogenous vs. heterogeneous population of OSNs. Ultimately, how exposure to different odors, specific for subsets of OSNs, may influence the process at this level remains to be determined.

Growth cones are specializations at leading edges of axons and dendrites as well as at sites of synaptogenesis. Devoto and Barnstable (1989) developed a mouse antibody to CDA 1, a growth cone specific epitope that they identified in the cortex and the OB. Thus, labeling with CDA 1 allows us to track the development of neural circuits in the OB.

We first confirmed that CDA 1 is present in mitral cells by immunohistochemical assay in primary OB cultures enriched for MCs. Furthermore, CDA 1 enabled us to

focus on dendritic circuits after we made the observation that *in vivo*, there is no CDA 1 expression in the ONL, thus suggesting that it is specific to dendritic growth cones.

The patterns of CDA 1 expression that we saw suggest radially oriented progression of dendritic development outwards from the innermost layer in the OB.

Glomeruli begin to emerge at P0 (Treloar *et al*., 1999) at which age most MC dendrites are still broadly spread; consistent with this is the observation that CDA 1 levels in the GL are high at P0 and then decrease significantly between P0 and P2, suggesting ongoing dendritic remodeling. Low, constant levels of CDA 1 expression at P2 and continuing through at least P8 reflect the fact that the glomeruli have formed and MC dendritic morphology has largely stabilized.

The differential expression of CDA 1 in the EPL suggests spatiotemporal variation in the maturation of dendritic circuits in the outer versus the inner sublaminae. One possible interpretation for this variation is the IAS, a network formed by TCs whose lateral dendrites are restricted to the oEPL. These TCs coordinate activity between isofunctional glomeruli in the medial and lateral aspects of each OB (Liu and Shipley, 1994; Belluscio *et al.*, 2002). Perhaps the greater level of CDA 1 staining in the oEPL at postnatal ages (P0 and P8) indicates the delayed development of the TCs of the IAS.

In summary, mitral cell dendrogenesis progresses through a sequence from a broadly distributed arbor of uniform supernumerary dendrites to a single apical dendrite targeting a single glomerulus and limited numbers of lateral dendrites restricted to EPL (figure 13).

A qualitative assessment of spatiotemporal patterns of dendritic development is possible with anti-CDA 1 antibody, which appears to be specific for growth cones in both

in vitro and *in vivo* assays. Using this marker in the GL and EPL, we show that dendritic development occurs at different rates across layers. CDA 1 expression attains highest levels in the EPL and the broadest time window of postnatal dendritic development occurs in the oEPL. Dendritic development in the oEPL persists at a constant rate from

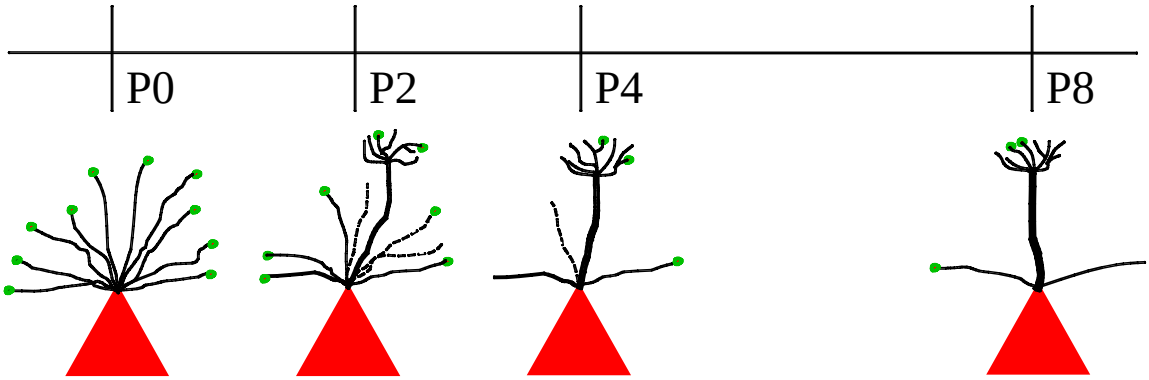

Figure 13. Schematic diagram of MC dendritic development combining results from DiI and CDA 1 experiments. At P0, the MC extends uniform supernumerary dendrites with growth cones at their leading edges dispersed throughout the GL and EPL. At P2, some of there are fewer supernumerary dendrites and one of these has emerged as the primary dendrite. Also at P2, CDA 1 expression has significantly decreased in the GL from P0, suggesting that the dendritic tuft is assuming the mature morphology. Furthermore, CDA 1 expression in the GL persists at this low level throughout the ages examined suggesting some degree of plasticity in the dendritic tuft. In addition, CDA 1 expression decreases significantly from P0 to P2 in the iEPL, where MC lateral dendrites are found, suggesting that lateral dendrite development is moving towards completion. At P4, we witness the emergence of the mature primary dendrite ending in a glomerular tuft and several lateral dendrites extending parallel to the surface of the OB in the iEPL. CDA 1 expression in the iEPL at this age decreases significantly from P2, and continues at a low level through P8, suggesting stabilization with perhaps some degree of plasticity.

P0 to P4 only decreasing significantly from initial postnatal levels by P8. Dendritic development in the iEPL and GL decreases significantly after P0. Dendritic development is more active in the oEPL at all ages as compared to the iEPL.

Recent results suggest that CDA 1 expression may persist at similar levels at P10, therefore an important future direction would be to extend CDA 1 analysis to later ages. In addition, future experiments to extend both the qualitative assessment using DiI and the quantitative analysis with CDA 1 to embryonic ages seem crucial. Finally, our preliminary results suggest temporal variation of CDA 1 expression along the

rostrocaudal axis. As a result, CDA 1 could also be used to extend the analysis to include the rostrocaudal and dorsoventral axes and thus elucidate spatiotemporal patterns of dendritic development along these axes.

REFERENCES

Ache BW, Young JM. Olfaction: diverse species, conserved principles. *Neuron*. 2005. 2005;48(3):417-430.

Allison A. The morphology of the olfactory system in the vertebrates. *Biol. Rev. Cambridge Philosophical Soc.* 1953;42:23-32.

Axel R. Scents and sensibility: a molecular logic of olfactory perception (Nobel lecture). *Angew. Chem. Int. Ed. Engl*. 2005;44:6110-6127.

Au WW, Treloar HB, Greer CA. Sublaminar organization of the mouse olfactory bulb nerve layer. *J. Comp. Neurol*. 2002;446:68-80.

Benson TE, Ryugo DK, Hinds JW. Effects of sensory deprivation on the developing mouse olfactory system: a light and electron microscopic, morphometric analysis. *J Neurosci*. 1984;4(3):638-653.

Belluscio L, Lodovichi C, Feinstein P, Mombaerts P, Katz LC. Odorant receptors instruct functional circuitry in the mouse olfactory bulb. *Nature*. 2002;419:296-300.

Brunjes PC, Greer CA. Progress and directions in olfactory development. *Neuron*. 2003;38(3):371-374.

Buck LB. Unraveling the sense of smell (Nobel lecture). *Angew. Chem. Int. Ed. Engl*. 2005;44:6128-6140.

Buck L, Axel R. A novel multigene family may encode odorant receptors: a molecular basis for odor recognition. *Cell*. 1991;65:175-187.

Buonviso N, Chaput MA. Response similarity to odors in olfactory bulb output cells presumed to be connected to the same glomerulus: electrophysiological study using simultaneous single-unit recordings. *J. Neurophysiol*. 1991;63:447-454.

Buonviso N, Chaput MA, Scott JW. Mitral cell-to-glomerulus connectivity: and HRP study of the orientation of mitral cell apical dendrites. *J. Comp. Neurol*. 1991;307:57-64.

Cajal SR. 1911. *Histologie du Système Nerveux de l'Homme et de Vertébrés*. Paris: Maloine.

Catania KC. Olfaction: Underwater 'sniffing' by semi-aquatic mammals. *Nature*. 2006;444(7122):1024-1025.

Chen WR, Midtgaard J, Shepherd GM. Forward and backward propagation of dendritic impulses and their synaptic control in mitral cells. *Science*. 1997;278(5337):463-467.

Cline HT. Dendritic arbor development and synaptogenesis. *Curr. Opin. Neurobiol*. 2001;11:118-126.

Crowley JC, Katz LC. Early development of ocular dominance columns. *Science*. 2000;290(5495):1321-1324.

Devoto SH, Barnstable CJ. Expression of the growth cone specific epitope CDA 1 and the synaptic vesicle protein SVP38 in the developing mammalian cerebral cortex. *J. Comp. Neurol*. 1989;290:154-168.

Feinstein P, Bozza T, Rodriguez I, Vassalli A, Mombaerts P. Axon guidance to glomeruli by odorant receptors and the β2 adrenergic receptor. *Cell*. 2004;117:833-846.

Feng G, Mellor RH, Bernstein M, Keller-Peck C, Nguyen QT, Wallace M, et al. Imaging neuronal subsets in transgenic mice expressing multiple spectral variants of GFP. *Neuron*. 2000;28(1):41-51.

Firestein S. How the olfactory system makes sense of scents. *Nature*. 2001;413(6852):211-218.

Fields RD, Neale EA, Nelson PG. Effects of patterned electrical activity on neurite outgrowth from the mouse sensory neurons. *J. Neurosci*. 1990;10:2950-2964.

Furrer MP, Kim S, Wolf B, Chiba A. Robo and frazzled/DCC mediate dendritic guidance locally at the CNS midline. *Nat. Neurosci*. 2003;6:223-230.

Gao FB, Brenman JE, Jan LY, Jan YN. Genes regulating dendritic outgrowth, branching, and routing in Drosophila. *Genes Dev*. 1999;13(19):2549-2561.

Graziadei PP, Monti-Graziadei GA. Neurogenesis and neuron regeneration in the olfactory system of mammals. I. Morphological aspects of differentiation and structural organisation of the olfactory sensory neurons. *J. Neurocytol*. 1979;8:1-18.

Greer CA, Stewart WB, Teicher MH, Shepherd GM. Functional development of the olfactory bulb and a unique glomerular complex in the neonatal rat. *J. Neurosci*. 1982;2:1744-1759.

Greer CA. Golgi analyses of dendritic organization among denervated olfactory bulb granule cells. *J. Comp. Neurol*. 1987;257(3):442-452.

Greer CA, Hálasz N. Plasticity of dendrodendritic microcircuits following mitral cell loss in the olfactory bulb of the murine mutant Purkinje cell degeneration. *J. Comp. Neurol*. 1987;256:284-298.

Guthrie KM, Anderson AJ, Leon M, Gall C. Odor-induced increases in c-fos messenger RNA expression reveal an anatomical unit for odor processing in the olfactory bulb. *Proc. Natl. Acad. Sci*. USA. 1993;90:3329-3333.

Hálasz N, Greer CA. Terminal arborizations of olfactory nerve fibers in the glomeruli of the olfactory bulb. *J. Comp. Neurol*. 1993;337:307-316.

Hinds JW. Early neuron differentiation in the mouse of olfactory bulb. I. Light microscopy. *J. Comp. Neurol*. 1972;146(2):233-252.

Hinds JW, Hinds PL. Reconstruction of dendritic growth cones in neonatal mouse olfactory bulb. *J. Neurocytol*. 1972;1:169-187.

Hinds JW. Early neuron differentiation in the mouse olfactory bulb. II. Electron microscopy. *J. Com.p Neurol*. 1972;146(2):253-276.

Hinds JW, Ruffett TL. Mitral cell development in the mouse olfactory bulb: reorientation of the perikaryon and maturation of the axon initial segment. *J. Comp. Neurol*. 1973;151(3):281-306.

Imamura F, Nagao H, Naritsuka H, Murata Y, Taniguchi H, et al. A leucine-rich repeat membrane protein, 5T4, is expressed by a subtype of granule cells with dendritic arbors in specific strata of the mouse olfactory bulb. *J. Comp. Neurol*. 2006;495(6):754-768.

Isaacson JS, Strowbridge BW. Olfactory reciprocal synapses: dendritic signaling in the CNS. *Neuron*. 1998;20(4):749-761.

Iwema CL, Fang H, Kurtz DB, Youngentob SL, Schwob JE. Odorant receptor expression patterns are restored in lesion recovered rat olfactory epithelium. *J. Neurosci*. 2004;24:356-369.

Jan YN, Jan LY. The control of dendrite development. Neuron. 40:229-42Johnson BA, Woo CC, Ninomiya-Tsuboi K, Leon M. 1996. Synaptophysin-like immunoreactivity in the rat olfactory bulb during postnatal development and after restricted early olfactory experience. *Dev. Brain Res*. 2003;92(1):24-30.

Jourdan F, Duveau A, Astic L,Holley A. Spatial distribution of [14C] 2-deoxyglucose uptake in the olfactory bulbs of rats stimulated with two different odours. *Brain Res*. 1980;188:139-154.

Kasowski HJ, Kim H, Greer CA. Compartmental organization of the olfactory bulb glomerulus. *J. Comp. Neurol*. 1999;407:261-274.

Keith CH, Wilson MT. Factors controlling axonal and dendritic arbors. *Int. Rev. Cytol*. 2001;205:77-147.

Kim H, Greer CA. The emergence of compartmental organization in olfactory bulb glomeruli during postnatal development. *J. Comp. Neurol*. 2000;422:297-311.

Kim S, Chiba A. Dendritic guidance. *Trend Neurosci*. 2004;27(4):194-202.

Kishi K, Mori K, Ojima H. Distribution of local axon collaterals of mitral, displaced mitral, and tufted cells in the rabbit olfactory bulb. *J. Comp. Neurol*. 1984;225:511-526.

Klenoff JR., Greer CA. Postnatal development of olfactory receptor cell axonal arbors. *J. Comp. Neurol*. 1998;390:245-260.

Leon M, Johnson BA. Olfactory coding in the mammalian olfactory bulb. *Brain Res. Brain Res. Rev*. 2003;42:23-32.

Lin DM, Wang F, Lowe G, Gold GH, Axel R, Ngai J, et al. Formation of precise connections in the olfactory bulb occurs in the absence of odorant-evoked neuronal activity. *Neuron*. 2000;26(1):69-80.

Lipscomb BW, Treloar HB, Greer CA. Novel microglomerular structures in the olfactory bulb of mice. *J. Neurosci*. 2002;22(3):766-774.

Lipscomb BW, Treloar HB., Klenoff, J, Greer CA. Cell Surface carbohydrates and glomerular targeting of olfactory sensory neuron axons. *J. Comp. Neurol*. 2003;467:22-31.

Liu WL, Shipley MT. Intrabulbar associational system in the rat olfactory bulb comprises cholecystokinin-containing tufted cells that synapse onto the dendrites of GABAergic granule cells. *J. Comp. Neurol*. 1994;346(4):541-558.

Lledo PM, Alonso M, Grubb MS. Adult neurogenesis and functional plasticity in neuronal circuits. *Nat. Rev. Neurosci*. 2006;7(3):179-193.

López-Mascaraque L, Garcia C, Valverde F A, De Carlos JA. Central olfactory structures in Pax-6 mutant mice. *Ann N Y Acad Sci*. 1998;855:83-94.

López-Mascaraque L, Garcia C, Blanchart A, De Carlos JA. Olfactory epithelium influences the orientation of mitral cell dendrites during development. *Dev. Dyn*. 2005;232:325-335.

Lovell P, Moroz LL. The largest growth cones in the animal kingdom: an illustrated guide to dynamics of Aplysia. *Integrative and Comparative Biology*. 2006;46(6):847-870.

Macrides F, Schneider SP. Laminar organization of mitral and tufted cells in the main olfactory bulb of the adult hamster. *J. Comp. Neurol*. 1982;208:419-430.

Malun D, Brunjes PC. Development of olfactory glomeruli: temporal and spatial interactions between olfactory receptor axons and mitral cells in opossums and rats. *J. Comp. Neurol*. 1996;368(1):1-16.

Matsutani S, Senba E, Tohyama M. Distribution of neuropeptide-like immunoreactivities in the guinea pig olfactory bulb. *J. Comp. Neurol*. 1989;280:577-586.

Matsutani S, Yamamoto N. Differentiation of mitral cell dendrites in the developing main olfactory bulbs of normal and naris-occluded rats. *J. Comp. Neurol*. 2000;418:402-410.

Meisami E, Noushinfar E. Early olfactory deprivation and the mitral cells of the olfactory bulb: a Golgi study. *Int. J. Dev. Neurosci*. 1986;4(5):431-444.

Miyamichi K, Serizawa S, Kimura HM, Sakano H. Continuous and overlapping expression domains of odorant receptor genes in the olfactory epithelium determine the dorsal/ventral positioning of glomeruli in the olfactory bulb. *J. Neurosci*. 2005;11:979-984.

Mombaerts P. Targeting olfaction. *Curr. Opin. Neurobiol*. 1996;6:481-486.

Mombaerts P, Wang F, Dulac C, Chao SK, Nemes A, *et al*. Visualizing an olfactory sensory map. *Cell*. 1996;87:675-86.

Mombaerts P. How smell develops. *Nat. Neurosci*. 2001;4 Suppl.:1192-1198.

Mombaerts P. The human repertoire of odorant receptor genes and pseudogenes. *Annu. Rev. Genomics Hum. Genet*. 2001;2:493-510.

Mombaerts P. Odorant receptor gene choice in olfactory sensory neurons: the one receptor-one neuron hypothesis revisited. *Curr. Opin. Neurobiol*. 2004;14:31-36.

Mombaerts P. Axonal Wiring in the Mouse Olfactory System. *Annu. Rev. Cell Dev. Biol*. 2006;22:713-737.

Mori K, Kishi K, Ojima H. Distribution of dendrites of mitral, displaced mitral, tufted, and granule cells in the rabbit olfactory bulb. *J. Comp. Neurol*. 1983;219(3):339-355.

Mori K, Nagao H, Yoshihara Y. The olfactory bulb: coding and processing of odor molecule information. *Science*. 1999;286(5440):711-715.

Nagayama S, Takahashi YK, Yoshihara Y, Mori K. Mitral and tufeted cells differ in the decoding manner of odor maps in the rat olfactory bulb. *J. Neurophysiol*. 2004;91:2532-2540.

Polleux F, Morrow T, Ghosh A. Semaphorin 3A is a chemoattractant for cortical apical dendrites. *Nature*. 2000;404(6778):567-573.

Rodriguez I, Feinstein P, Mombaerts P. Variable patterns of axonal projections of sensory neurons in the mouse vomeronasal system. *Cell*. 1999;97(2):199-208.

Royet JP, Souchier C, Jourdan F, Ploye H. Morphometric study of the glomerular population in the mouse olfactory bulb: numerical density and size distribution along the rostrocaudal axis. *J. Comp. Neurol*. 1988;270:559-568.

Sato Y, Hirata T, Ogawa M, Fujisawa H. Requirement for early-generated neurons recognized by monoclonal antibody lot1 in the formation of lateral olfactory tract. *J. Neurosci*. 1998;18(19):7800-7810.

Schoenfeld TA, Marchand JE, Macrides F. Topographic organization of tufted cell axonal projections in the hamster main olfactory bulb: an intrabulbar associational system. *J. Comp. Neurol*. 1985;239:378-391.

Schoppa NE, Kinzie JM, Sahara Y, Segerson TP, Westbrook GL. Dendrodendritic inhibition in the olfactory bulb is driven by NMDA receptors. *J. Neurosci*. 1998;18(17):6790-6802.

Schoppa NE, Westbrook GL. Glomerulus-specific synchronization of mitral cells in the olfactory bulb. *Neuron*. 2001;31(4):639-651.

Sestan N, Rakic P, Donoghue MJ. Independent parcellation of the embryonic visual cortex and thalamus revealed by combinatorial Eph/ephrin gene expression. *Curr Biol*. 2001;11(1):39-43.

Shepherd GM. The Human Sense of Smell: Are We Better Than We Think? *PLoS Biol*. 2004;2(5):e146.

Shepherd GM, Chen WR, Greer CA. 2004. Olfactory Bulb. In: GM Shepherd (ed). *The Synaptic Organization of the Brain*, 5th ed., pp.165-216. New York: Oxford University Press.

Shipley MT, Ennis M. Functional organization of olfactory system. *J. Neurobiol*. 1996;30:123-176.

Stewart WB, Kauer JS, Shepherd GM. Functional organization of rat olfactory bulb analyzed by the 2-deoxyglucose method. *J. Comp. Neurol*. 1979;185:715-734.

Takami S, Graziadei PP. Light microscopic Golgi study of mitral/tufted cells in the accessory olfactory bulb of the adult rat. *J. Comp. Neurol*. 1991;311(1):65-83.

Treloar HB, Purcell AL, Greer CA. Glomerular formation in the developing rat olfactory bulb. *J. Comp. Neurol*. 1999. 413;289-304.

Treloar HB, Feinstein P, Mombaerts P, Greer CA. Specificity of glomerular targeting by olfactory sensory axons. *J. Neurosci*. 2002;22:2469-2477.

Treloar HB, Gabeau D, Yoshihara Y, Mori K, Greer CA. Inverse expression of olfactory cell adhesion molecule in a subset of olfactory axons and a subset of mitral/tufted cells in the developing rat main olfactory bulb. *J. Comp. Neurol*. 2003;458:389-403.

Wachowiak M, Shipley MT. Coding and synaptic processing of sensory information in the glomerular later of the olfactory bulb. *Semin. Cell Dev. Biol*. 2006;17(4):411-423.

Walz A, Mombaerts P, Greer CA, Treloar HB. Disrupted compartmental organization of axons and dendrites within olfactory glomeruli of mice deficient in the olfactory cell adhesion molecule, OCAM. *Mol. Cell. Neurosci*. 2006;32:1-14.

Wang F, Nemes A, Mendelsohn M, Axel R. Odorant receptors govern the formation of a precise topographic map. *Cell*. 1998;93(1):47-60.

Whitford KL, Marillat V, Stein E, Goodman CS, Tessier-Lavigne M, et al. Regulation of cortical dendrite development by slit-robo interactions. *Neuron*. 2002;33:47-61.

Wong RO, Ghosh A. Activity-dependent regulation of dendritic growth and patterning. *Nat. Rev. Neurosci*. 2002;3:803-812.

Wu G, Cline HT. Stabilization of dendritic arbor structure in vivo by CAMKII. *Science*. 1998;279(5348):222-226.

Xue GP, Calvert RA, Morris RJ. Expression of the neuronal surface glycoprotein Thy-1 is under post-transcriptional control, and is spatially regulated, in the developing olfactory system. *Development.* 1990;109(4):851-864.

Yokoi M, Mori K, Nakanishi S. Refinement of odor molecule tuning by dendrodendritic synaptic inhibition in the olfactory bulb. *Proc Natl Acad Sci* USA. 1995;92(8):3371-3375.

Zhang X, Firestein S. The olfactory receptor gene superfamily of the mouse. *Nat. Neurosci*. 2002;5:124-133.

Zheng C, Feinstein P, Bozza T, Rodriguez I, Mombaerts P. Peripheral olfactory projections are differentially affected in mice deficient in a cyclic nucleotide-gated channel subunit. *Neuron*. 2000;26(1):81-91.

Zou DJ, Feinstein P, Rivers AL, Mathews GA, Kim A, *et al*. Postnatal refinement of peripheral olfactory projections. *Science*. 2004;304:1976-1979.

Zou Z, Horowitz LF, Montmayeur JP, Snapper S, Buck LB. Genetic tracing reveals a stereotyped sensory map in the olfactory cortex. *Nature*. 2001;414:173-179.